This is a repository copy of *Local head loss monitoring using acoustic instrumentation in partially full sewer pipes*.

White Rose Research Online URL for this paper:
http://eprints.whiterose.ac.uk/95120/

Version: Accepted Version

Article:
Romanova, A., Tait, S. and Horoshenkov, K.V. orcid.org/0000-0002-6188-0369 (2012) Local head loss monitoring using acoustic instrumentation in partially full sewer pipes. Water Science and Technology, 65 (9). pp. 1639-1647. ISSN 0273-1223

https://doi.org/10.2166/wst.2012.058

Reuse
Unless indicated otherwise, fulltext items are protected by copyright with all rights reserved. The copyright exception in section 29 of the Copyright, Designs and Patents Act 1988 allows the making of a single copy solely for the purpose of non-commercial research or private study within the limits of fair dealing. The publisher or other rights-holder may allow further reproduction and re-use of this version - refer to the White Rose Research Online record for this item. Where records identify the publisher as the copyright holder, users can verify any specific terms of use on the publisher's website.

Takedown
If you consider content in White Rose Research Online to be in breach of UK law, please notify us by emailing eprints@whiterose.ac.uk including the URL of the record and the reason for the withdrawal request.

eprints@whiterose.ac.uk
https://eprints.whiterose.ac.uk/

Local head loss monitoring using acoustic instrumentation in partially full sewer pipes

A. Romanova, S. Tait and K. V. Horoshenkov

School of Engineering Design and Technology, University of Bradford, Great Horton Road, Bradford, West Yorkshire, BD7 1DP, UK
(E-mail: *a.romashk@gmail.com*)

Abstract After an increase in capital investment in UK sewers to reduce hydraulic capacity problems, the proportion of sewer flooding incidents now linked to blockages has increased. It is clear that if sewer operators are to continue to reduce flooding incidents, then better blockage management is now required. Sewer blockage formation is poorly understood, blockages are intermittent and occur in a number of circumstances. This paper reports on the development of low cost acoustic instrumentation that can identify the location of a pipe blockage and then estimate the local head loss as a result of the presence of a blockage. A set of experiments were carried out in two full scale laboratory pipes. The pipes' condition was altered by inserting blockages of different sizes. Acoustic data was recorded and presented in terms of the acoustic energy reflected from the partially blocked pipe. The results of this study show that the total reflected acoustic energy correlates with the measured head loss. A new empirical relation between the reflected acoustic energy and head loss due to a blockage is derived. This knowledge can then be used to estimate the reduction in flow capacity resulting from a blockage based on a single remote measurement.

Keywords Reflected acoustic energy; sewer pipe; friction factor; local head loss; flow capacity

INTRODUCTION

In the UK the underground sewer system totals some 300,000 km in length. Water companies need enhanced information on sewers to manage efficiently their day-to-day performance. The operational condition of sewer systems can change over time due to blockages caused by sediment and fats. The incidence of pipe blockage has been linked to flooding and other service failures. Currently, it is very difficult to gather sufficient timely information on the condition of a sewer pipe to pro-actively prevent hydraulic failure due to blockage.

In the UK flooding caused by hydraulic overload has been progressively tackled through capital investment, 'flooding other causes' has now become an increasingly significant mode of service failure. Analysis by Arthur et al. (2008) showed that in England and Wales, there were around 25,000 sewer blockages of which 13% resulted in internal property flooding. Water companies are therefore now looking for new ways of reducing these incidents through means such as modelling to identify blockage 'hot-spots', and CCTV inspection to locate developing blockage problems, followed by pro-active sewer jetting.

In contrast to flooding due to hydraulic overload, 'flooding other causes' problems commonly exist on small diameter local sewers, which make up by far the largest proportion of any sewer network. Given this fact it is not sufficient to focus inspection resources on the 20% or so of 'critical' sewers as is the current recommended guidance (WRc, 2010). Current visual inspection technologies, developed to identify structural failures are limited by cost and time, different technology is needed that will work quickly and economically to identify the presence of blockages and then estimate the impact that this can have on the flow capacity of individual pipes. Furthermore, the inspection and cleansing required is not a one-off activity. Having identified areas at risk it is important to regularly check for progressive blockage development and intervene again at the right time, before flow capacity deteriorates to a level that flooding occurs. Traditional CCTV techniques are not the

ideal means of doing this, being relatively slow and expensive. As a result, a better alternative is required to provide information on the presence of a blockage and its impact on pipe flow.

Blanksby et al. (2002) carried out an analysis of historical water company customer complaints and mapped this onto CCTV records to examine the causes of flooding incidents over a range of sewer sizes. Their study indicated that the majority of flooding incidents were in smaller sewers, and that the majority of these were caused by intermittent blockages rather than structural failures. The analysis also indicated that collapses were proportionately more prevalent in smaller sewers, but that the incidence of structural problems was low with around only 2% of the CCTV surveyed lengths showing signs of structural deterioration. They concluded that it would be difficult to generate a pro-active cleaning routine based on prior predictions as the data indicated that the location of blockages generally could not be linked to a structural defect and so was thought to be linked with either the local hydraulic conditions, or sources of high levels of silt and fat inputs. It appears that continual monitoring may provide a better answer to managing sewer blockages rather than some predictive tool due to the intermittent nature of the processes that are involved in pipe blockage formation.

Several modelling approaches have been developed in order to predict the likelihood of occurrence of sewer blockages and failure. Savic et al. (2006) used data-driven techniques to derive statistical relationships to predict the likelihood of sewer blockage for different pipe classes. They used data from asset and customer complaint databases to develop and demonstrate these relationships. These techniques do not however identify individual locations within a catchment but indicated raised risk of blockage formation in pipes with particular characteristics. Arthur et al. (2008) examined the statistical significance between pipes with a high incidence of observed blockage and various factors. The study used data from a small catchment and considered each failure separately. The selected catchment had an existing sewer network model and hydraulic outputs from this model were combined with incidents in a customer complaints database. Analysis indicated that the risk of blockage was related to predicted locations of flooding and low flow velocities, it was also shown that there was a statistical link to enhanced blockage formation in smaller sewers.

In spite of these computational approaches, the need for direct inspection to identify sewer blockages is clear due to the intermittent nature of blockage development and the inability to clearly identify the location of individual blockages. This paper reports on the development of a low cost sensor system that can identify the location of a sewer pipe blockage and then estimate the local head losses due to the blockage.

CONCEPTUAL FRAMEWORK

Hydraulic elements – head loss due to walls and local losses

The history of friction factor estimation dates back to the mid 19th century. In 1857, Darcy and Weisbach (Moody, 1944) established a strong correlation of energy loss in full-flowing pipes due to wall friction effects:

$$h_f = f\frac{L}{D}\frac{V^2}{2g} \qquad (1)$$

Where h_f is the head loss due to pipe wall friction, f is the dimensionless Darcy-Weisbach friction factor coefficient, L is the pipe length, D is the pipe diameter, V is the average flow velocity g is the acceleration due to gravity. It should be noted that this equation should only be used for full pipes with steady-state, turbulent flow. For the laboratory experiments described below, partially full pipes (pipes with free surfaces) were used, so the Darcy – Weisbach friction factor is presented in terms of hydraulic radius (R) instead of pipe diameter:

$$f = \frac{8gRs_f}{V^2} \quad (2)$$

Where s_f is the friction slope and is equal to pipe bed slope, for pipes with free surface, steady, uniform flow conditions present in a pipe without any blockage. In the case of a pipe with non-uniform flow conditions created by a blockage the following technique for obtaining an estimate of the local head loss (specific energy loss), h_f at the blockage was used:

$$f = \frac{8gR}{V^2}\frac{h_f}{L_{2-1}} \quad (3)$$

$$h_f = \left(\frac{V_1^2}{2g} + h_1 + z_1\right) - \left(\frac{V_2^2}{2g} + h_2 + z_2\right) \quad (4)$$

Where h_f is the local specific energy loss V_1 and V_2 are the experimentally estimated cross-section average velocities at the pipe locations upstream and downstream sections of the section containing the blockage respectively. Hence, h and z are the experimentally measured water depths and pipe elevations and their value of the measured local flow depth and flow rate can be used to calculate the local mean flow velocities. By estimating the local energy loss and its position then it is possible to calculate the reduction in flow capacity in any pipe caused such a the local energy loss.

Acoustic elements – reflected energy

We will attempt to link the local head loss discussed in the previous section with the acoustic energy reflected in pipes that contain a blockage. The acoustic energy can be obtained from the reflected acoustic intensity, from a signal produced by a single source, and measured by a pair of microphones.

The acoustic intensity is a vector quantity with the direction identical to sound wave propagation (Jacobsen, 1991). The time-dependent acoustic pressure responses recorded by a pair of microphones, $p_1(t)$ and, $p_2(t)$ which are separated by known distance Δ, the instantaneous intensity vector is described by the following equation:

$$I(t) = p(t)u(t) \approx \frac{p_1(t)+p_2(t)}{2\Delta\rho_0}\int[p_1(t) - p_2(t)]dt \quad (5)$$

where $\vec{u}(t) = -\frac{1}{\rho_0}\int\frac{\partial p}{\partial \vec{n}}dt$ is the acoustic velocity vector, n is the normal with identical direction to sound propagation, $\rho_0 = 3.432 \times 10^{-3}\frac{p_a}{T}$, T is the temperature in Kelvins, and p_a is the current atmospheric pressure.

The acoustic pressure responses recorded on a pair of microphones were used to calculate the instantaneous acoustic intensity according to the method detailed above. The instantaneous intensity was filtered in a narrow frequency band and presented as a function of the distance $d = tc_0$, where t is the time and c_0 is the sound speed in air. A separate temperature probe was used to determine the temperature in the pipe. This temperature value was used to calculate accurately the sound speed from the following expression$c_0 = 343.2\sqrt{T/293}$, (Bies & Hansen, 2003).

The sign which the instantaneous intensity takes determines the direction in which the sound energy propagates. Here it is assumed that the negative sign of the intensity corresponds to the incident (outgoing) wave radiated by the speaker and the positive sign corresponds to the reflections which return from the pipe containing the blockage to the microphone array.

The above instantaneous intensities were used to determine the energy content in the recorded acoustic data for a range of pipe conditions. For this purpose the intensity data taken from the six microphone pairs were normalized so that the intensity minimum corresponding to the incident sound wave was set to $min\{I(t)\} = -1$ for all measured data. The positive part of the intensity corresponds to that reflected from cross-sectional changes that occur in the pipe. The total reflected acoustical energy in the wave reflected in the direction of the sensor can then be determined from the following expression:

$$ET = \frac{1}{2}\int_{t\ min}^{t\ max}\{|I(t)| + I(t)\}dt \quad (6)$$

Effectively, integral (6) includes the reflected energy which occurs due to the pipe wall roughness and the blockage present in the pipe.

EXPERIMENTAL APPARATUS

The experiments were conducted in two different full scale sewer pipes located in the Hydraulics Laboratory at the University of Bradford. One pipe was a sloping 24m long clay pipe with circular cross section of 150mm in diameter. The pipe was constructed from a number of 615mm long clay pipe sections with sealed socket type connections. The bed slope of this circular pipe was fixed at 0.01 for all experiments. This represents a realistic slope in the field for small diameter sewers. The pipe was divided into three sections. The upstream section is 5m long which allows the flow regime to fully develop to form uniform conditions. The middle section is 14m long which is the experimental part containing the blockage, has an entry in the top of the pipe where model blockages will be placed to simulate a local roughness. The entry does not change the pipe cross-sectional shape. The downstream section is also 5m long and it serves to separate the experimental flow section from the outlet pipe effect. A second series of experiments were conducted in a sloping inclined 20m long plastic pipe with circular cross section of 290mm in diameter. This pipe was constructed from a number of 2000mm long sections with sealed socket type connections. The bed slope of the plastic pipe was also fixed at 0.01 for all experiments. This pipe had an entry at the top of the pipe at 9m from the pipe inlet so that different models could be placed at this location to simulate local head losses.

Cast concrete models were used as surrogate blockages to simulate local obstructions and to introduce a local flow roughness to the flow. The model blockages took the form of a sector of a circle and were placed in the pipe invert. The models were made from a sand and cement mixture. For the 150mm pipe, the model samples were 100mm long (L_m) and ranged in height (B) 15mm, 30mm, 40mm, 55mm, and 60mm to represent the pipe cross-sectional area blocked (A_B) of 10% to 40% of the original pipe cross-sectional area. For the 290mm pipe, the model samples were 200mm long and had heights (B) of 20mm, 30mm, 40mm, 50mm, 60mm, 70mm, 90mm, and 110mm. This provided a pipe cross-sectional area blocked from 7% to 38% of the original pipe cross-sectional area.

The concept of the measurement method is to measure reflected acoustic energy, this is reflected from a range of artefacts within a pipe e.g., joints and wall roughness, as well as any discrete blockage and the resulting water level profile. Two different pipes (clay with joints and plastic with minimal joints) were used so that the influence of joint construction and pipe wall material could also be examined.

Hydraulic procedures

In each test a steady discharge, controlled by an upstream butterfly valve located in the inlet pipe to each test pipe, was introduced and maintained. At the downstream end of each pipe the time to fill a tank of a known volume was used to determine the volumetric flow rate. In each pipe, three

experimental steady flow regimes were used with discharges (Q) of 0.42 l/s, 1 l/s and 1.8 l/s for the 150mm diameter pipe and 3 l/s, 13 l/s and 32 l/s for 290mm diameter pipe. These flow rates resulted in a uniform water depth (h) of 17mm, 23mm, 32mm for the 150mm diameter pipe and 31mm, 63mm, 98mm for the 290mm diameter pipe, in the absence of the model obstructions. This ensured that similar proportions of area obstruction were achieved in both pipes for these hydraulic conditions. In the experiments with no blockages the uniform depth was determined when the water slope equalled the bed slope. The water depth along each pipe was monitored by the use of non-equidistantly spaced piezometers. In experiments with blockages, the majority of the piezometers readings were gathered before and after the blockage so as to provide accurate data on the streamwise water depth variation caused by the local obstruction. The local water level data was used to calculate the local velocity given the measured flow rate and the geometry of each pipe.

Acoustic procedures

Once the required hydraulic conditions had been achieved, the acoustic sensor was inserted into the pipe and attached to the soffit of the pipe at either the upstream or downstream end. The acoustic sensor contained a speaker and microphone array that were oriented towards the opposite end of the pipe. The sensor was connected via a coaxial cable to a laptop (Horoshenkov et al., 2008). A MatLAB code was written to generate a chirp sound through a 4-channel VX-Pocket soundcard. The output was amplified and emitted by the speaker. The emitted signal was reflected from any blockage in the pipe, detected by the 4-microphone array, digitised by the sound card and deconvolved using the laptop so that the acoustic pressure impulse response of the pipe could be determined. The distances between the microphone pairs were chosen to be much smaller than the wavelength (Horoshenkov et al., 2009). The sum of all microphone pairs was used to determine the acoustic intensity (Fahy, 1995). All of the acoustic measurements were repeated at least three times. Acoustic data was collected for flow conditions with and without blockages. In total, 36 experimental conditions were examined.

RESULTS

Hydraulic data

The experimentally measured hydraulic data conditions for the 150mm and 290mm diameter pipes with and without the presence of the model blockages are presented in Table 1.

In this table, the model blockage heights are labelled as B. The values of the measured water depth used to estimate head loss caused by the blockage (h_f) were located immediately upstream of the blockage (location 1, h_1) and downstream of the blockage where the water returns to uniform flow conditions (location 2, h_2) For the 150mm pipe the water depth measurement points one and two were located at 6.5m and 12.1m and the downstream face of the block was located at 7.1m from the pipe inlet. For 290mm pipe the points were located at 8.91m and 14.6m and the downstream face of the block was located at 9.2m from the pipe inlet.

Recorded water level at point one (h_1) and point two (h_2) were used to calculate the local hydraulic conditions to determine the Reynolds numbers (Re_1 and Re_2), local Froude Number (Fr_1 and Fr_2) and the local head loss associated with the blockage, see eqn. 4. From the values of Froude number at location 2 it can be seen that in all the experiments the flows downstream of the blockages were in the supercritical flow regime, so that there is no hydraulic jump effect after the blockage. The head loss h_f estimated the head loss due to flow over the blockage and as the flow regain its uniform depth.

The ratios of blockage height just upstream of the blockage to pipe diameter (h_1/D) and the blockage area to pipe cross-sectional area (A_B/A_p) are presented in last columns of Table 1.

Table 1. Measured hydraulic conditions and ratios for all experiments.

Flow regime	**D** mm	***Q*** l/s	***B*** mm	h_1 mm	h_2 mm	Re_1 -	Re_2 -	Fr_1 -	Fr_2 -	h_f m	h_1/D -	A_B/A_p -
1	150	0.42	0	17	17	14294	14294	1.13	1.13	0.056	0.11	-
2	150	0.42	15	32	17	10223	14294	0.32	1.13	0.065	0.21	0.052
3	150	0.42	30	44	17	8575	14294	0.17	1.13	0.076	0.29	0.142
4	150	0.42	40	51	17	7884	14294	0.13	1.13	0.083	0.34	0.214
5	150	0.42	55	66	17	6767	14294	0.08	1.13	0.098	0.44	0.332
6	150	0.42	60	73	17	6357	14294	0.07	1.13	0.105	0.49	0.374
7	150	1	0	23	23	29044	29044	1.48	1.48	0.056	0.15	-
8	150	1	15	35	23	23180	29044	0.65	1.48	0.056	0.23	0.052
9	150	1	30	52	23	18562	29044	0.30	1.48	0.069	0.35	0.142
10	150	1	40	60	23	17066	29044	0.23	1.48	0.077	0.40	0.214
11	150	1	55	74	23	15006	29044	0.15	1.48	0.090	0.49	0.332
12	150	1	60	80	23	14272	29044	0.13	1.48	0.096	0.53	0.374
13	150	1.8	0	32	32	43811	43811	1.39	1.39	0.056	0.21	-
14	150	1.8	15	34	32	42390	43811	1.23	1.39	0.055	0.23	0.052
15	150	1.8	30	64	32	29551	43811	0.36	1.39	0.069	0.43	0.142
16	150	1.8	40	73	32	27244	43811	0.28	1.39	0.078	0.49	0.214
17	150	1.8	55	87	32	24296	43811	0.20	1.39	0.091	0.58	0.332
18	150	1.8	60	94	32	23027	43811	0.17	1.39	0.098	0.63	0.374
19	290	3	0	31	31	54441	54441	1.74	1.74	0.057	0.11	-
20	290	3	20	62	31	37724	54441	0.44	1.74	0.060	0.21	0.030
21	290	3	30	75	31	33989	54441	0.31	1.74	0.072	0.26	0.055
22	290	3	40	81	31	32565	54441	0.26	1.74	0.077	0.28	0.083
23	290	3	50	94	31	29938	54441	0.20	1.74	0.089	0.32	0.115
24	290	3	60	102	31	28562	54441	0.17	1.74	0.097	0.35	0.149
25	290	13	0	63	63	162056	162056	1.86	1.86	0.057	0.22	-
26	290	13	40	123	63	110789	162056	0.51	1.86	0.052	0.42	0.083
27	290	13	50	147	63	99175	162056	0.36	1.86	0.072	0.51	0.115
28	290	13	60	157	63	95033	162056	0.32	1.86	0.081	0.54	0.149
29	290	13	70	167	63	91203	162056	0.28	1.86	0.090	0.58	0.186
30	290	13	90	188	63	83954	162056	0.23	1.86	0.109	0.65	0.264
31	290	13	110	210	63	77201	162056	0.18	1.86	0.130	0.72	0.348
32	290	32	0	98	98	311789	311789	1.94	1.94	0.057	0.34	-
33	290	32	60	205	98	193668	311789	0.47	1.94	0.050	0.71	0.149
34	290	32	70	222	98	181560	311789	0.40	1.94	0.063	0.77	0.186
35	290	32	90	250	98	162496	311789	0.31	1.94	0.088	0.86	0.264
36	290	32	110	276	98	143350	311789	0.22	1.94	0.112	0.95	0.348

*h_f for a pipe without a blockage the head loss is estimated between location 1 and 2 according to eqn 4.

The water depth data for the one of the flow rate conditions (Q=0.42 l/s) in the 150mm diameter pipe is shown in Figure 1. The figure clearly demonstrates that the water depth is uniform for the flow condition without a model blockage. However, with the introduction of blockages of different sizes, it can be noted, that the trend for the water depth increases significantly upstream of the blockage and rapidly decreases immediately downstream the block. The above water level behaviour is recognised for all experiments with a pipe blockage.

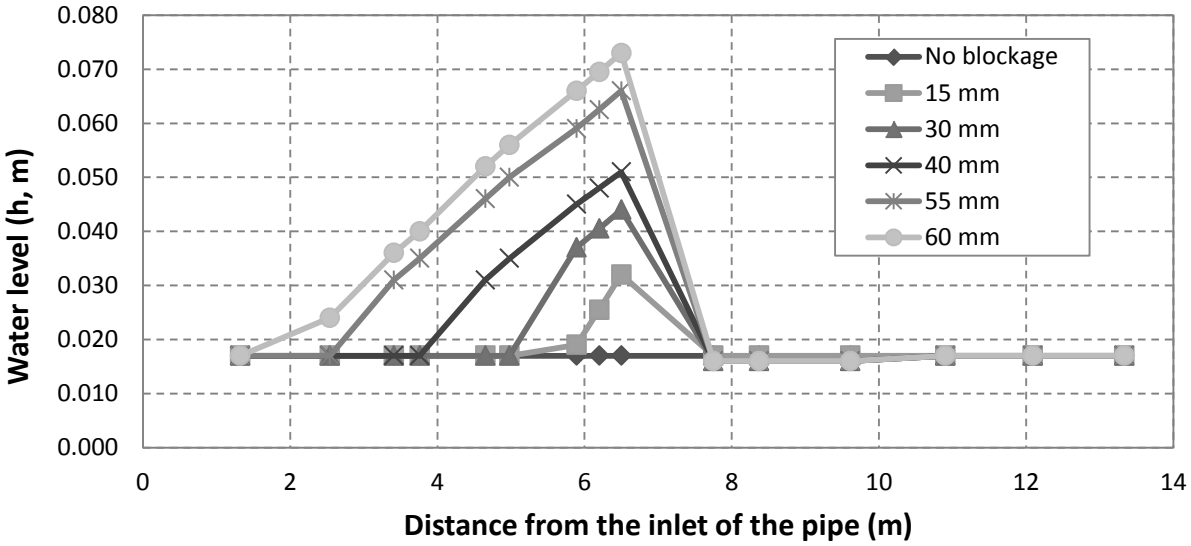

Figure 1. Water depth values for clean and blocked pipe for flow discharge of Q=0.42 l/s, pipe diameter 150mm.

Local energy loss

Figure 2 illustrates the effect of blockages with increasing height (h_m) on the streamwise pattern of total energy for one flow rate. The total energy at locations were calculated using the local flow depths, the measured flow rate and the measured pipe slope. The figure shows error bars associated with bed slope and water depth measurements – these were estimated from the standard deviation from repeated water depth measurements. This indicated that an error of 5% of the measured water depth was reasonable. Due to the model blockage, the water depth increased upstream of the blockage, where the energy loss with streamwise distance is minimal. It is clear that the local energy loss at the blockage is dependent on the blockage height if the flow rate is maintained.

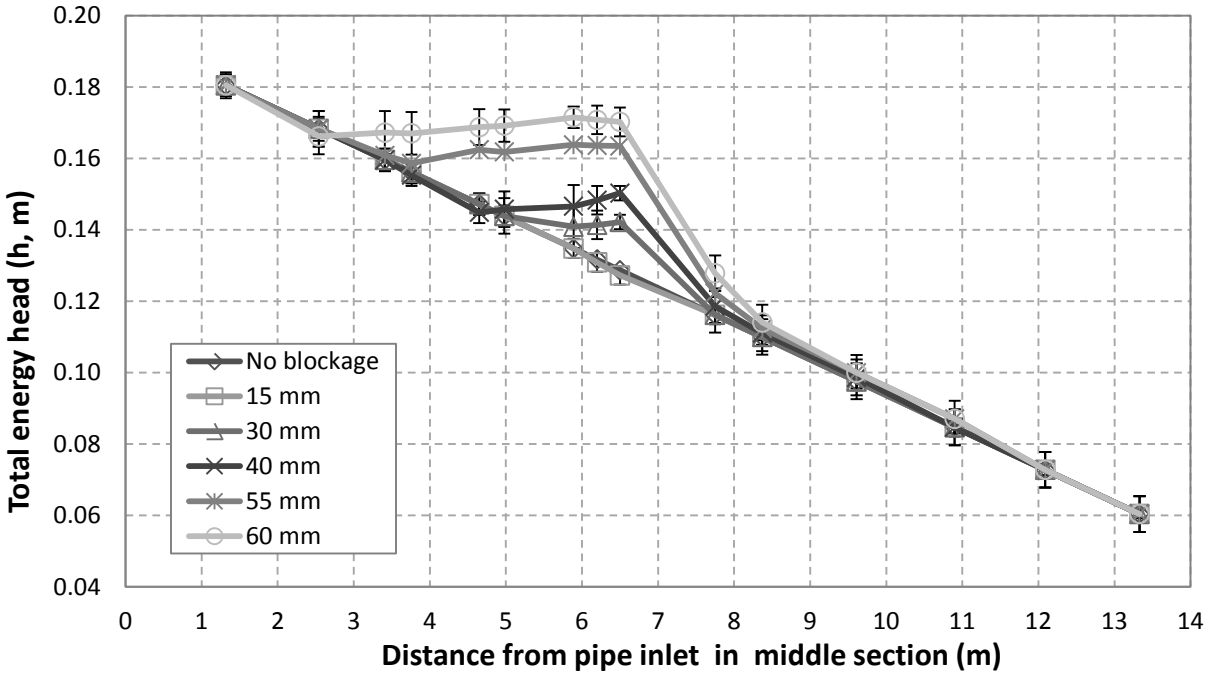

Figure 2. Effect of blockage height on energy head for flow discharge of Q=1.8 l/s, pipe diameter 150mm.

Table 2 presents the local head loss and acoustic energy data for all experimental conditions, as well as the generalised forms for these parameters.

A non-dimensional value of head loss in relation to the head loss for the same section of clean pipe ($(h_f - h_f^C)/h_f^C$) is presented in of table 2. The head loss for a clean pipe condition is denoted as h_f^C, which was calculated from equation 4. The acoustic energy (ET) was calculated for the all the experiments and analysed in the frequency range of 100 - 750 Hz. The presented acoustic energy is the least mean square values of upstream and downstream readings from all the repeated experiments. A non-dimensional acoustic energy value ($(\mathrm{ET} - \mathrm{ET}_0)/\mathrm{ET}_0$) relative to a clean pipe conditions is presented in the Table 2. ET_0 is the acoustic energy content for the same pipe and discharge (uniform velocity), although without the presence of a blockage. This was done so that the influence of reflections from joints and pipe wall roughness could be removed from the analysis. The term $(\mathrm{ET} - \mathrm{ET}_0)/\mathrm{ET}_0$ therefore represents the amount of additional reflected energy relative to that reflected in a clean pipe with the same flow discharge.

The negative non-dimensional head loss values appear for three flow regime cases (Table 2) for the smallest block. These values appear due to the overall 4% error of water depth readings.

Examining the data in table 2 it is clear that when even the smallest blockage (7% of pipe cross-sectional area) is introduced into the pipe the measured amount of reflected energy is always at least 180% larger than the measurement when there was no blockage. The data also indicates that the level of reflected energy increases with increasing discharge in both pipes but the level if increased is negligible in comparison with the increases observed when blockages are introduced into the pipe. It is therefore clear that the increases in the level of reflected energy observed when blockages are used is significantly higher than the levels associated with pipe wall and joint condition and the flowing water.

Table 2. Measured hydraulic and acoustic conditions for all experiments.

Flow regime	**D** mm	***Q*** l/s	***B*** mm	h_f m	$(h_f - h_f^C)/h_f^C$ -	***ET*** -	$(ET - ET_0)/ET_0$ -
1	150	0.42	0	0.056	0.00	0.205	0
2	150	0.42	15	0.065	0.16	0.593	1.9
3	150	0.42	30	0.076	0.36	0.962	3.7
4	150	0.42	40	0.083	0.48	1.300	5.3
5	150	0.42	55	0.098	0.75	2.633	11.8
6	150	0.42	60	0.105	0.87	3.371	15.4
7	150	1	0	0.056	0.00	0.247	0
8	150	1	15	0.056	0.00	0.789	2.2
9	150	1	30	0.069	0.24	1.461	4.9
10	150	1	40	0.077	0.37	1.991	7.1
11	150	1	55	0.090	0.61	3.409	12.8
12	150	1	60	0.096	0.72	4.518	17.3
13	150	1.8	0	0.056	0.00	0.300	0
14	150	1.8	15	0.055	-0.03	1.284	3.3
15	150	1.8	30	0.069	0.24	2.301	6.7
16	150	1.8	40	0.078	0.39	2.840	8.5
17	150	1.8	55	0.091	0.62	5.465	17.2
18	150	1.8	60	0.098	0.74	6.436	20.5
19	290	3	0	0.057	0.00	1.126	0
20	290	3	20	0.060	0.06	2.950	1.6
21	290	3	30	0.072	0.26	3.491	2.1
22	290	3	40	0.077	0.35	4.068	2.6
23	290	3	50	0.089	0.57	4.886	3.3
24	290	3	60	0.097	0.70	6.348	4.6
25	290	13	0	0.057	0.00	1.561	0

26	290	13	40	0.052	-0.08	7.578	3.9
27	290	13	50	0.072	0.26	10.807	5.9
28	290	13	60	0.081	0.41	12.047	6.7
29	290	13	70	0.090	0.57	15.000	8.6
30	290	13	90	0.109	0.92	28.000	12.1
31	290	13	110	0.130	1.29	37.000	20.0
32	290	32	0	0.057	0.00	2.000	0
33	290	32	60	0.050	-0.13	18.000	8.0
34	290	32	70	0.063	0.11	22.000	10.0
35	290	32	90	0.088	0.54	36.000	17.0
36	290	32	110	0.112	0.97	44.000	21.0

Acoustic spectrogram

To identify the frequency-dependent behaviour of the reflected intensity and those sections of the pipe that caused these reflections to occur, intensity spectrograms were produced as shown in Figure 3 for all the tests. Darker areas in these spectrograms correspond to stronger acoustic reflections, whereas white areas correspond to sections of the pipe that caused little or no reflections.

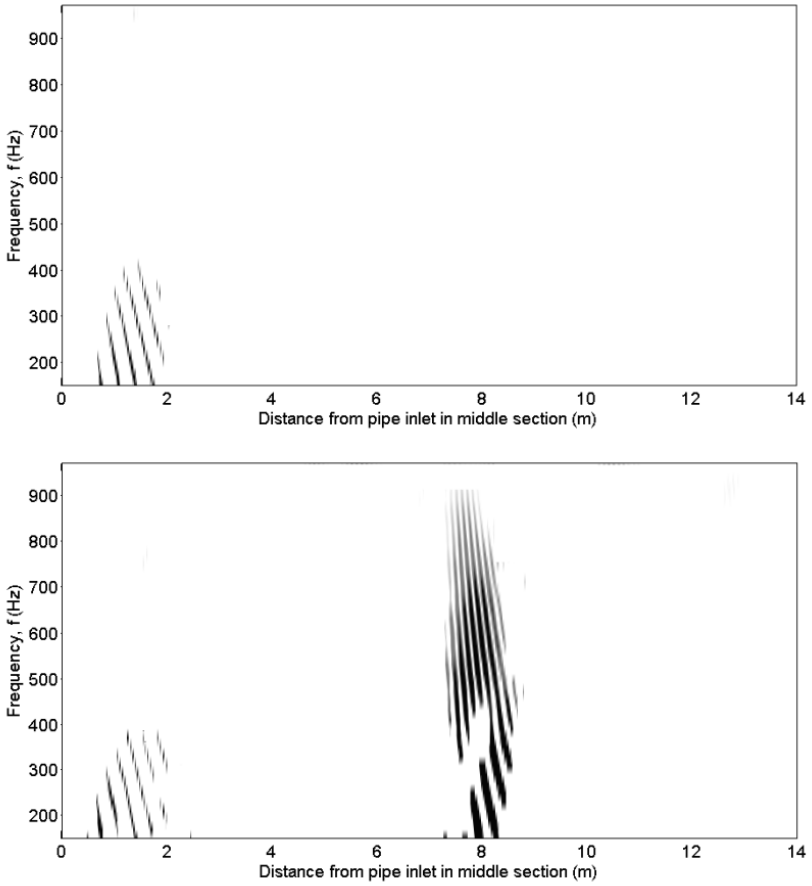

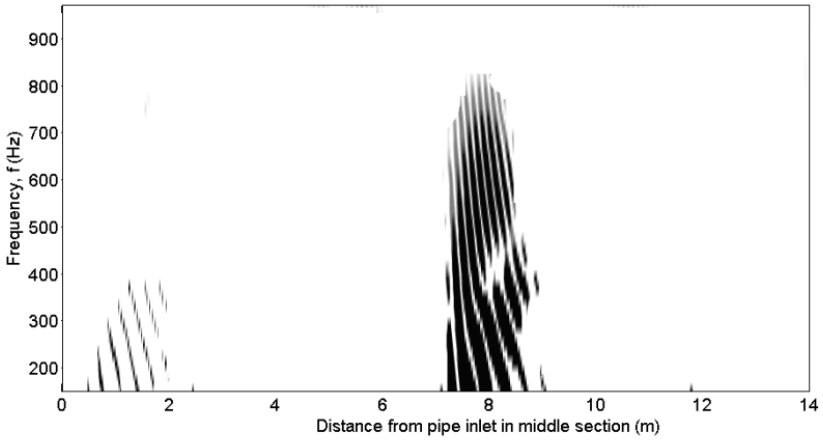

Figure 3. Intensity spectrogram from pipe downstream end for no blockage and with 15mm and 55mm high blockage for 1 l/s discharge in a 150mm diameter pipe (top to bottom).

Figure 3 demonstrates that for an increase in obstruction height (reflection from an obstacle at 7m) results in an increase in the strength of the reflected signal for the range of frequencies selected. For empty pipe conditions (no blockage), but with the presence of water, no energy reflection in any of the selected frequency range occurs. Small reflections visible at 0.5m corresponds to a poor joint connection in the 150mm pipe. In this paper, the reported values of reflected energy correspond only to reflections caused by the blockage placed at 7m in the 150mm diameter pipe.

Relation of acoustic monitoring to hydraulic elements

The links between various hydraulic parameters, the non-dimensional reflected acoustic energy and the non-dimensional geometric measures of the blockages was explored. The non-dimensional relative acoustic reflected energy $(ET - ET_0)/ET_0$ was found to be related with geometrical parameters such as blockage height to pipe diameter, and blockage area to pipe area (Figure 4). It is clear the measured acoustic response is responsive to all the geometric parameters in figure 4. There is slightly more scatter in the water depth to pipe diameter data for the 290mm diameter pipe that the 150mm diameter pipe.

By examining the results further, figure 5 and 6 shows the dependence of the non-dimensional reflected acoustic energy on the non-dimensional hydraulic local energy loss calculated by eqn. 4 for 150mm pipe and 290mm pipe. Both of the pipes follow a similar pattern for all the experiments, where the data is dependent on flow discharge and pipe size. These dependencies are expressed as exponential functions and have R^2 values, calculated in the accepted form between 0.97 to 0.99. There are slightly better correlations between the hydraulic energy loss and the acoustic data than the geometrical changes and the acoustic data. The above results indicate that, the prediction of pipe geometrical parameters due to the blockage and the local head loss caused by a blockage is valid for a range of relative blockage sizes (7-40% of the original pipe cross-sectional area) and in pipes with different diameters and joint conditions for a range of flow rates and joint conditions. The acoustic measurement method can therefore be used to estimate the size and location of a local energy loss and so with limited additional calculation this information can be used to determine the reduction in flow capacity in pipe caused by a single blockage. This information can also be imported into a sewer hydraulic network model to characterise a local energy loss so can aid the modelling of the impact of a real blockage on localised flooding.

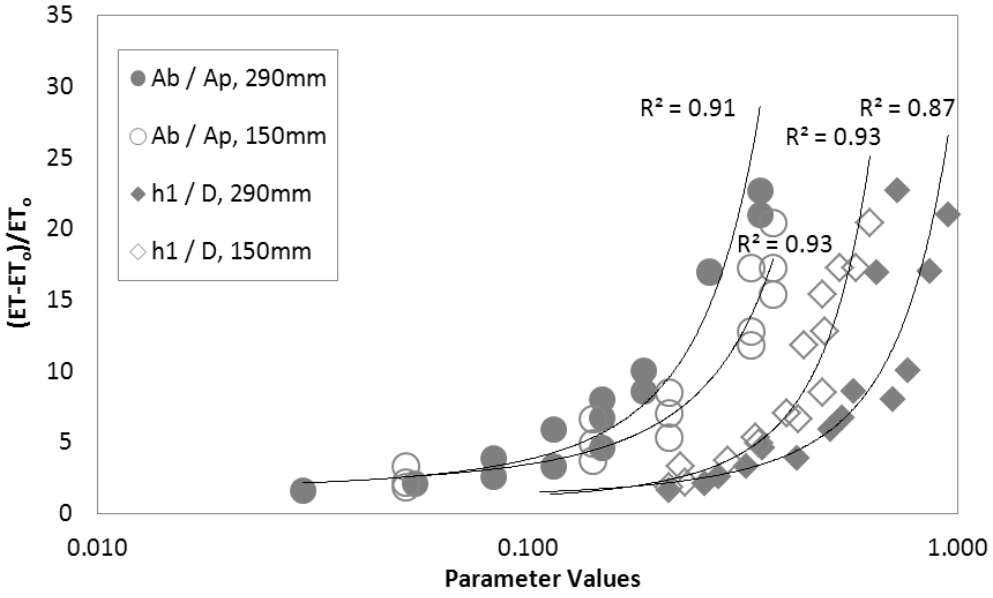

Figure 4. Non-dimensional relative acoustic energy to blockage/pipe geometry parameters.

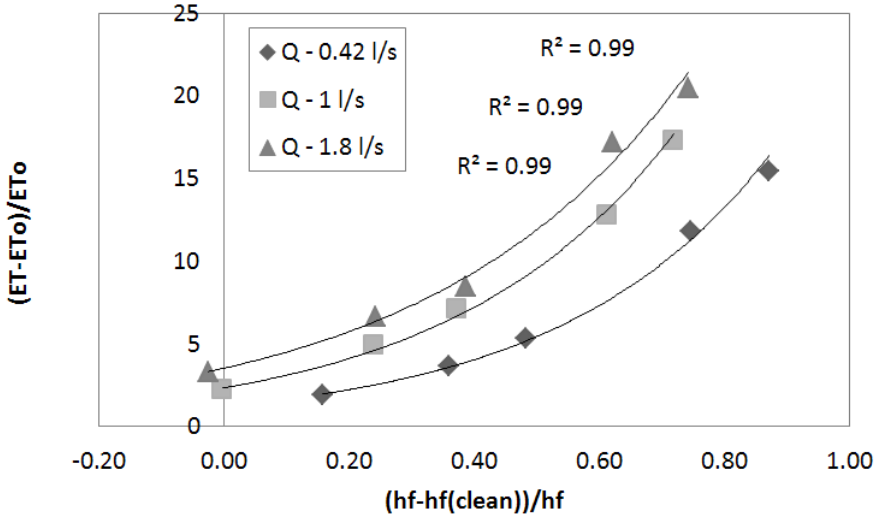

Figure 5. Acoustic total energy to hydraulic energy head loss relation for 150mm diameter pipe.

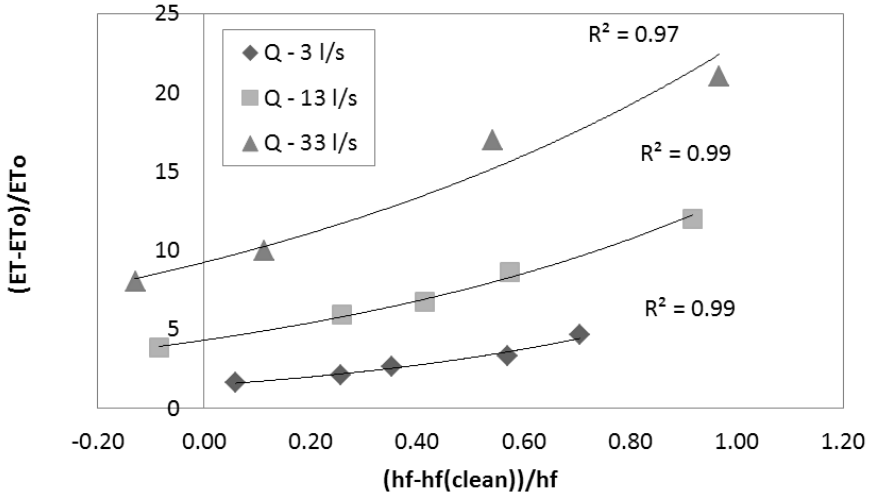

Figure 6. Acoustic total energy to hydraulic energy head loss relation for 290mm diameter pipe.

CONCLUSIONS

A series of laboratory experiments were carried out in order to demonstrate that instrumentation could be developed that could identify the location of pipe blockages, estimate the local energy losses caused by that blockage and so provide data that could be used to estimate the impact of that blockage on pipe flow capacity. A low cost acoustic sensor consisting of a low power speaker and four microphones was manufactured and used to measure the total reflected energy in two laboratory pipes of different diameter, wall material and joint configuration. A series of systematic experiments were conducted in which the head loss and total reflected acoustic energy were measured for a range of differently sized pipe blockages at different flow rates. The data indicated that as the blockage size increased local head losses increased, and that as the water depth was increased for a fixed blockage size the local energy losses decreased. This corresponded with previous work. By considering the whole data set it was shown that the acoustic energy can be used to determine directly the local hydraulic energy loss caused by a single blockage in a pipe for a range of blockage sizes and flow conditions. This estimate of head loss, and the location of the blockage can be related and can then be used to estimate the reduction in pipe flow capacity caused by the presence of a single blockage. A simple empirical relationship was proposed. The measurement method appears to be insensitive to reflections caused by pipe wall and joint conditions and from the free surface of the water in a partially filled pipe.

Given that the acoustic energy can be independently measured either from upstream or downstream end of the pipe and involves measurements that take only tens of seconds to accomplish, the use of a simple acoustic sensor located within a pipe can therefore be used to track the development of a blockage within a combined or stormwater sewer pipe. The use of such simple sensing technology offers the opportunity for sewer network manager to pro-actively monitor developing blockages and so act in a timely fashion before such blockages cause such a large reduction in flow capacity that sewer flooding occurs. The use of such sensors allows for the continual monitoring of blockage development that is not possible using existing numerical models of sewer networks or inspection techniques.

REFERENCES

Arthur S., Crow H., Pedezert L. (2008) Understanding Blockage Formation in Combined Sewer Networks, Water Management, 161, 215-221.

Bies, D. A. & Hansen, C. H. (2003) Engineering noise control: Theory and practice. 3rd edn., London: Spon Press.

Blanksby J., Khan A., Jack A. (2002) Assessment of cause of blockage of small diameter sewers. Proc. Int. Conf. On Sewer Operation and Maintenance, ISBN 1 851 432 132.

Fahy, F. (1995). Sound Intensity, London: Elsevier 1995.

Horoshenkov, K. V, Tolstoy, A., Bin Ali, M. T. (April 2009). Detecting pipe changes via acoustic matched field processing. Applied Acoustics (Elsevier), 70 (5), 695-702.

Horoshenkov, K.V, Tait, S. J., Bin Ali, M. T., Long, R. (August 2008). Patent Application: Improvements in and Relating to Apparatus for the Airborne Acoustic Inspection of Pipes. GB081519905.

Jacobsen, F. (1991) A note on instantaneous and time-averaged active and reactive sound intensity. Journal of sound and vibration, 147(3), pp.489-496.

Moody, L.F. (1944). "Friction Factors for Pipe Flow". Transactions of the ASME 66 (8): 671–684.

Savic D., Giustolisi O., Berardi L., Shepherd W., Djordjevic S. (2006) Modeling Sewer Failure by Evolutionary Computing, Water Management , 159, 111-118.

WRC (2010) Sewerage Rehabilitation Manual, 4th Edition online - http://srm.wrcplc.co.uk, accessed 4th July 2011, WRc Swindon.